npj Computational Materials

www.nature.com/npjcompumats

ARTICLE OPEN

Check for updates

A graph based approach to model charge transport in semiconducting polymers

Ramin Noruzi[1,3], Eunhee Lim[2,3], Balaji Sesha Sarath Pokuri[1,3], Michael L. Chabinyc[2]✉ and Baskar Ganapathysubramanian[1]✉

Charge transport in molecular solids, such as semiconducting polymers, is strongly affected by packing and structural order over several length scales. Conventional approaches to modeling these phenomena range from analytical models to numerical models using quantum mechanical calculations. While analytical approaches cannot account for detailed structural effects, numerical models are expensive for exhaustive (and statistically significant) analysis. Here, we report a computationally scalable methodology using graph theory to explore the influence of molecular ordering on charge mobility. This model accurately reproduces the analytical results for transport in nematic and isotropic systems, as well as experimental results of the dependence of the charge carrier mobility on orientation correlation length for polymers. We further model how defect distribution (correlated and uncorrelated) in semiconducting polymers can modify the mobility, predicting a critical defect density above which the mobility plummets. This work enables rapid (and computationally extensible) evaluation of charge mobility semiconducting polymer devices.

npj Computational Materials (2022)8:38 ; https://doi.org/10.1038/s41524-022-00714-w

INTRODUCTION

Predicting the charge carrier mobility of semicrystalline polymers is challenging because of the interplay between ordered and disordered regions[1,2]. Polymer chains in ordered regions are extended with long conjugation lengths and packed such that the interchain electronic coupling is weak, but still significant for charge transport. The chains in the amorphous regions have a significantly broader distribution of electronic couplings between neighboring chains due to structural disorder. In the ordered regions, transport may occur through extended electronic states whereas in the disordered regions charges are thought to move by hopping between localized sites[3,4]. The ability of high resolution transmission electron microscopy (HR-TEM)[5–11] and X-ray scattering methods[12–14] to reveal the detailed morphology of semiconducting polymers presents an opportunity to reveal how ordered and disordered regions impact charge transport. The challenge is to model how charge transport occurs between these two regions, which can guide the design of new polymers and processing routes to achieve higher carrier mobilities.

The level of detail in models of charge transport in polymers has a significant influence on their applicability. For crystalline polymers, quantum mechanical calculations can be performed to predict the band structure of perfectly ordered chains and thereby model the mobility of carriers in ordered regions[3,15]. Disordered, or amorphous, polymers can be difficult to model using such techniques and can require very large scale simulations that combine molecular dynamics to model molecular-scale morphologies and electronic structure calculations on specific microstructures[16–19]. Most semiconducting polymers have a mixture of ordered and disorder domains leading to challenges in incorporating both types of regions in transport models. Hopping models that consider transport between localized steps as a set of jumps between sites on model lattices have been widely used. Energetic disorder is incorporated by varying the distribution of the energies of the sites that charges jump between[4]. While such lattice models are powerful, it can be difficult to model systems with spatial anisotropies over long ranges relative to the spacing of sites. Hopping simulations can additionally require computationally intensive methods, such as kinetic Monte Carlo (kMC) techniques, that can constrain the ability to study experimentally relevant time and length scales[20,21]. While there has been recent success in running such models at device scales[22], performing design or parametric exploration using such approaches remains intractable. More importantly, the addition of molecular level detail can obscure the general behavior, i.e. they may be too materials specific to reveal critical behavior[23,24].

A simple model for understanding the difference in behavior of transport in amorphous and crystalline polymers considers the competition of transport along a polymer chain and between chains[25]. By defining a timescale for diffusion along a chain and a timescale for hopping between chains, the behavior of amorphous and nematic polymers can be modeled analytically. In real systems, the landscape for charge transport is more complex with energetic disorder within both ordered and disordered regions, a distribution of chain lengths, and varying connectivity between ordered and disordered regions. However, this coarse model of competition between transport along a chain and between chains captures much of the essential physics of transport in polymers.

Recently, there has been significant progress in developing more realistic models to understand how charges move through the complex morphological landscape of polymers[24,26,27]. Tie chains that connect ordered domains through amorphous regions have been recognized as an important factor in transport[1,14,28–30]. For example, in poly(3-hexylthiophene) (P3HT) the crystallites are ~20 nm along the chain axis and if the disordered domains are of similar dimensions, then an extended chain of ~150 repeat units can span two domains as a tie chain. Using a description from polymer mechanics of the number of tie chains, the charge carrier mobility of P3HT was studied by addition of higher MW polymer

[1]Mechanical Engineering, Iowa State University, Ames, IA, USA. [2]Materials Department, University of California, Santa Barbara, CA, USA. [3]These authors contributed equally: Ramin Noruzi, Eunhee Lim, Balaji Sesha Sarath Pokuri. ✉email: mchabinyc@engineering.ucsb.edu; baskarg@iastate.edu

to a lower MW matrix revealing that low percentages of tie chains can greatly enhance the charge carrier mobility in field effect transistors[31]. Efficient analytical models for transport that consider the role of electronic defects, i.e. kinks in tie chains, that would cause charge trapping have also been developed[30]. By combining a model for the role of defects with coarse models of the alignment of ordered domains, limits were found for when transport within ordered domains dominates and when defects dominate[30]. Other models incorporating percolation and hopping transport using numerical simulations of morphologies generated by coarse grain molecular modeling have also been reported[32]. Hopping-based models that use MC methods are computationally intensive for large scale studies, i.e. over statistically large numbers of morphologies or large length scales[33]. For example, kMC simulations have been reported to model transport in transistors by considering length scales of ~1 micron in the transport direction, but only ~10 nm in the transverse directions[22]. Three-dimensional modeling over significant length scales with computational efficiency remains very challenging[34]. Therefore, there is still a need for efficient models that capture factors beyond tie chains including the distribution of chain lengths (molecular weight), energetic disorder and the varying connectivity of ordered regions that are becoming experimentally accessible.

Here we report on an approach that uses graph theory to model charge transport and percolation in semiconducting polymers as a function of their morphology. Graph theory is particularly appealing for modeling transport as it enables (a) abstracting out material specific details into a small set of features (graph edge weights, graph connectivity, graph node color), thus allowing generalization, (b) utilization of sophisticated, highly optimized graph algorithms that enable computationally efficient assessment of large systems, and (c) natural extensions to account for more complex effects like chain length distribution, energetic disorder and varying connectivity. Graph methods have been used previously in organic electronics to study transport in molecular solids both in ordered and disordered structures[35–38].

In this work, we utilize a directed graph representation[39] to relate the spatial distribution of molecular chains in the organic solid with charge transport. Representation of morphology as a graph enables[40,41] us to efficiently (and exhaustively) identify all charge transfer pathways, and characterize their statistical features. Our graph based model is computationally inexpensive and simultaneously takes into account coexistence of crystalline and amorphous regions, the local orientation of the polymer chains, inter-chain and intra-chain hopping, and presence (and spatial distribution) of impurities. More importantly, such graph models can naturally account for information (hopping rates, overlap integrals, etc.) from detailed molecular calculations that are performed off-line. After representing the morphology of the organic solid as a directed graph, we associate the edges of the graph with properties related to charge hopping. We first consider the expected contributions of intrachain and interchain transport to hopping transport. The interchain transport will be anisotropic and will vary based on the respective orientation of two neighboring polymer chains (equivalently, set of graph nodes). We expect the electronic coupling between two co-linear polymer chains separated by their chain ends will be weak and act as an impediment to transport. Two side-by-side chains where their conjugated backbones are co-facially arranged will be coupled electronically allowing hopping between chains. If the chains are separated by their sidechains, then the electronic coupling will be weak preventing charge from hopping from one chain to the next. Additionally carriers can potentially hop between chains beyond nearest neighbors with the range being dependent on temperature and the energy of the site. Intrachain transport will be affected by the ordering of the polymer chain; extended chains have better electronic coupling than those with disordered conformations between repeat units. Therefore transport in ordered regions will be more efficient along chains than in disordered regions. Extended chains that bridge two ordered regions through the disordered regions are referred to as tie chains; it is presumed that transport along tie chains is comparable to that in the ordered domain. A graph model naturally capture these features by associating edge weights (electronic couplings) that represent interchain and intrachain transport.

Our graph-based model for transport is effectively a coarse-grain representation of the polymer solid. We represent the conjugated polymer chains as a collection of short connected rods, with each rod representing the local orientation of the

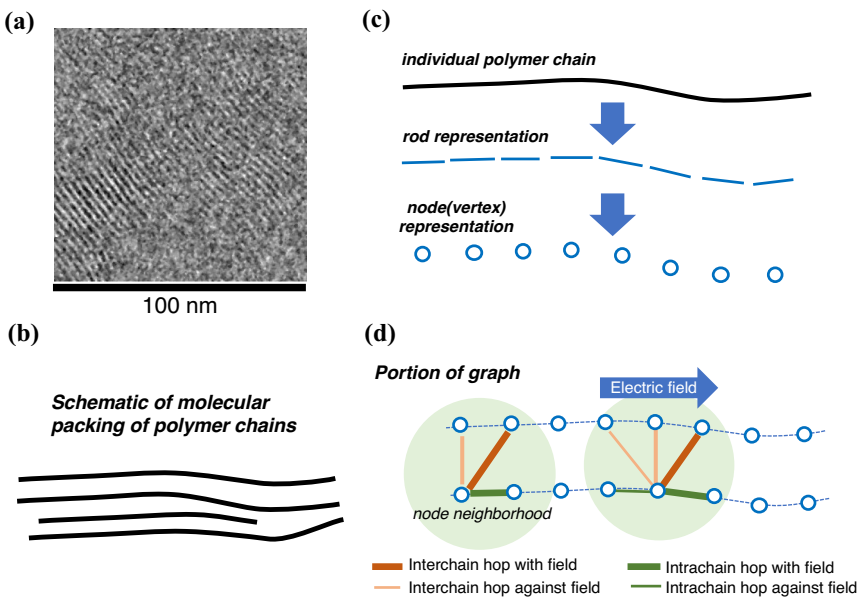

Fig. 1 Schematic illustration of the graph-based charge transport model. The model takes in an HRTEM image, identifies local order of polymer chains, represents with nodes to form a graph network which is then used to represent charge transport along a specified electric field direction.

backbone of the corresponding polymer chain (see Fig. 1). We convert this collection of rods into an equivalent graph representation[39,42]. Here, each rod is represented as a set of vertices arranged in order. We define two type of vertices (crystalline or amorphous vertices) and two types of edges that connect the vertices (intra-chain or inter-chain edges). The definition of the edge (and its weight, the edge weight) is directly related to charge transport (or charge hopping). Two vertices are connected by an edge if it is possible for a charge to hop between them, and the weight of the edge (i.e. strength of the connection) is proportional to the time duration for hopping (inversely proportional to the hopping frequency). Vertices that are considered to be part of the same polymer chain have edges that are weighted based on whether they are in crystalline or amorphous regions, where the weight increases the timescale for hopping in the amorphous region. The weights of the edges that connect vertices that belong to different polymer chains, i.e. intermolecular transport, are weighted differently than the edges of a polymer chain and by their relative orientation (to model the anisotropic electronic coupling) and the distance between the vertices. The weighting parameters were chosen to represent differences in the electronic coupling, e.g. a weight of 1 is the strongest coupling and larger weights represent weaker coupling. The weighting scheme is detailed in the "Methods" section. In our simulation, we have ignored variation in the site energies of the vertices, but the variation in weights between the chains captures part of the disorder.

Graph transport algorithms[43,44] then make it trivially simple to evaluate the effective charge transport between all vertices (hopping sites) mediated by the edges (which have different weights). By representing the network as a graph, effective charge transport can be equivalently looked as shortest paths between the respective electrodes (represented as electrode nodes in the graph). Edges with lower hop probability have higher weights, so that path is less preferred in the calculation of the shortest path between electrodes. We consider the shortest (weighted) path as the most probable path between a set of electrode nodes. Paths with higher total cumulative edge weights pass through low charge hop probability sites. Consequently, these will have lower mobilities compared to paths that have lower cumulative edge weights. The shortest path is analogous to the time taken by a charge to traverse the domain between this node pair. We find out the distribution of these weighted shortest paths for a large set of node pairs. The inverse of this distribution (scaled by the domain length) provides an estimate (in arbitrary units) of the mobility. By considering a large set of pairs of nodes across the morphology boundary, we construct a distribution of shortest paths which produces a mobility distribution. It should be noted that the distribution of graph shortest paths is one strategy of evaluating the mobility distribution. An alternative approach is to use graph flow algorithms to construct the max flow (of charges) through a morphology. Both provide similar abstractions of charge transport, and result in similar trends.

RESULTS

Comparison to analytical models

To help validate the graph-based model for transport, we first compare our results to those from an analytical model using a model for rigid rods. The effect of polymer chain length and molecular orientation on charge mobility was modeled analytically by Pearson and Pincus[25] and recently re-investigated using a similar approach[45]. Their model assumed one value for the time for a charge to diffuse along the extent of a polymer chain and one value of the time to hop between chains. Using these two parameters, the mobility of fully disordered Gaussian coil chains or nematic rods were determined. The mobility of a polymer chain

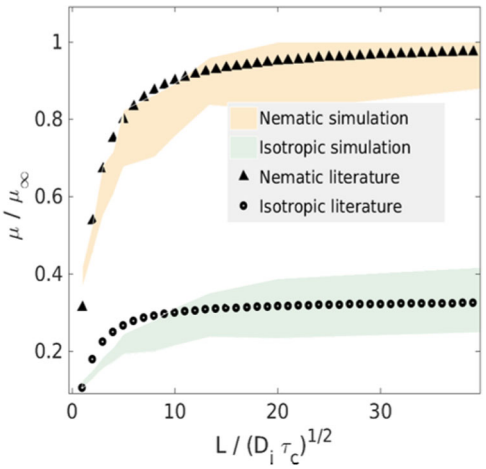

Fig. 2 Relative charge carrier mobility as a function of the length of the rod. The triangles represent the analytical solution for perfectly oriented rods and the circles represent isotropic orientation; the colored bands represent the range of the values from the graph-based model. The mobility has been non-dimensionalized with the mobility of an infinitely long rod that is perfectly oriented along the conduction axis and the length was non-dimensionalized with the distance, $(D_i\tau_c)^{1/2}$, a charge would diffuse on an infinitely long rod in a time τ_c.

with length L is

$$\mu(a) = \mu_\infty(\coth(a) - 1/a) = \mu_\infty \mathcal{L}(a) \quad (1)$$

where μ_∞ is the mobility of an infinite polymer chain and a is the length of a polymer chain (L) divided by the distance a charge career would diffuse in a time τ_c, on a chain of infinite length, $a = \frac{L}{(D_i\tau_c)^{1/2}}$. The operator $\mathcal{L}(a)$ is the Langevin function. We can mimic this calculation using our graph-based model by averaging over a large number of 2D microstructures. To model the cases with an analytical solution, we formed 100 microstructures with varying gaps between the end vertices of polymer chains and the given length of the chain. The number of simulations are chosen such that increasing the number of distinct microstructures does not lead to substantial changes in the range of results. Figure 2 plots the (normalized) mobility computed from our graph-based model and the analytical prediction for nematic and isotropic rods. Each microstructure gives a different mobility that results in the range shown in Fig. 2. The graph model captures the trend of the analytical model. We attribute the deviations for smaller length rods to the differing assumptions about the variation in coupling (edges between vertices) between nodes that does not perfectly replicate the simpler case of only two time constants.

Domain orientation and mobility

The graph-based model provides a means to examine more complex morphologies than analytical models, but without incurring large computational costs. For example, the length scale of alignment of ordered domains of polymers plays an important role in charge transport. The alignment allows chains to span aggregated or crystalline domains providing a pathway for charges to move between them; as the angle between domains increases then the polymer chains will become disordered if they tie domains together or the ties will be broken leading to inefficient charge transport[29]. One experimental metric for the length scale of alignment of polymer backbones is the orientational correlation length (OCL), which is defined as the average length over which domains with ordered polymer chains drift out of alignment with each other[12]. The OCL can be extracted from polarized soft X-ray scattering[12] or from electron microscopy

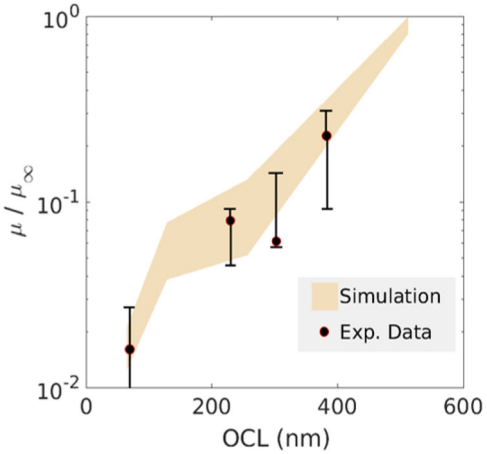

Fig. 3 A simulation of the relationship between mobility and orientational correlation length (OCL) of domains in a semicrystalline polymer when there is no substantial amorphous region between crystallites. The experimental data (with error bars) for the carrier mobility is for PBTTT from literature[12]. The carrier mobility is normalized with respect to the value at the maximum OCL—512 nm.

images[10]. The simple OCL metric has been shown to be correlated with carrier mobility of semiconducting polymers determined using thin film transistors[12,46] and also the bulk electrical conductivity of doped materials[47]. Figure 3 shows that the charge carrier mobility from thin film transistors of a thienothiophene-based polymer, PBTTT, follow an exponential relationship with the OCL[12]. Similar behavior was also observed for films that were electrically doped supporting that the OCL[47], which is a bulk measurement, tracks the behavior of charge carriers in the material. At the molecular weights and polydispersities used for the experimental data, we expect that tie chains should connect aligned domains and likely make the orientation the dominant factor in slowing transport. The graph model was used to evaluate the normalized mobility for length scales of the OCL using 100 model microstructures where no significant amorphous material between domains is present. In this analysis, the model microstructure consists of aligned polymer chains spaced regularly at a given distance between each other. In order to simulate the effect of OCL, circular regions of prescribed OCL size are rotated to a random angle, such that the mean angle over the domain is zero. Each of the polymer backbone is represented by nodes in a graph, and the weights are so chosen that difficult pathways (for e.g., inter-chain hops, grain boundary hops and hops as the orientation of domains changes.) are less favored over pathways with high electron mobility (for e.g., intra-chain hops). Further discussion on the model morphology and choosing physically coherent weights is presented in the "Methods" section. The predicted mobility varies by more than an order of magnitude and follows the exponential relationship with the OCL. The agreement with the experiment data suggests that the model captures the essential features that control transport.

Effect of defects on mobility

The behavior of the graph-based model shows good agreement with the comparable analytical model and shows good agreement with experimental data even using relatively simple assumptions. A powerful application of the graph-based approach is the ability to rapidly examine the influence of structure and defects, i.e. sites that are electronic traps or structural impediments to transport, on long range charge transport. Analytical approaches do not readily allow a distribution of morphologies and defects to be examined and KMC-based methods are inefficient due to limitations of the size of the regions that can be modeled. Here we readily modify the properties of the edges in the graph to model the role of defects on charge transport.

To fully quantify the effect of defects on mobility, we consider two broad types of defects—uncorrelated point defects, e.g. a trap at a node, and structural defects, e.g. imperfect chain lengths in crystalline regions, that exhibit a finite size. A graph-based approach makes it very simple to account for both types of defects and could also be extended to other types of structural defects, e.g. chains that loop back at domain boundaries. For a region of the morphology denoted as a defect, we simply modify the weight of the edges (i.e. hopping frequency) connecting the graph nodes associated with that region. The amount of the decrease in the hopping frequency can be turned to explore the effect of varying charge transport rates between pristine and defect regions on the effective mobility over longer ranges. Figure 4 shows this change as a function of changing the percentage of defects and their correlation using a model morphology. Each added defect to the morphology disables charge transport represented by the edges between nodes in that region, thereby constricting the flow of charges. The structural defects are incorporated by using Gaussian random fields[48]. From Fig. 4, it can be seen that in both cases, 1% is the critical density for the defects, and mobility decreases dramatically when density of defects is more than 1% of polymer chains. For both cases, the mobility decreases as the density of defects increases, but with a different dependence. The mobility drops as the density of defects increases in the uncorrelated case, but the drop is less dramatic at higher defect concentrations. Such behavior is reminiscent of the variation in materials like poly(3-hexylthiophene) that have relatively small ordered domains that have a ≈100× difference in variation of mobility between their crystalline (regioregular) and noncrystalline (regio-random) forms. Despite the defects, there is generally a pathway for charges to move through the graph. The drop in mobility is steeper with increasing correlated defects (panel b). If the defective regions are large (>5% defect ratio, with about ~5% domain size) then the carriers cannot find an effective pathway and are impeded. This result points out that defects that are aggregated into larger regions can lead to a larger disruption than if they are spread out spatially. This is quantified for a representative case in Fig. 4c.

Finally, Fig. 5 illustrates the behavior of the effective charge mobility as a function of both defect density as well as the ratio of the inter-chain to intra-chain hopping ratio. Each data point represents results from evaluating 500 microstructures, with a specific defect density and inter/intra chain mobility characteristics. For this study, we incorporate uncorrelated defects to the standard base-case morphology, similar to Fig. 4a. The complete dataset—consisting of around 15,000 simulations—took about 14 h (overnight) to evaluate on a standard desktop machine. In contrast, most alternate methods will take a substantially larger computation effort and time for comparable microstructures. The results show a very similar negative logarithmic dependence of the effective mobility with defect density. We also observe that the effect of an additional defect is much larger when the inter- and intra-chain hopping rates are similar. This can be attributed to the fact that when intrachain hopping rates are much higher than the interchain hopping rates, then the charge already prefers to take the path with minimum interchain hops. So, an added defect is only detrimental when it is precisely on one of the fastest pathway—the defect will modify the fastest pathway to include additional inter-chain hop in place of a much faster intra-chain hop. So, we can expect an average linear behavior as intra-chain hopping rates become larger and larger compared to inter-chain hopping rates.

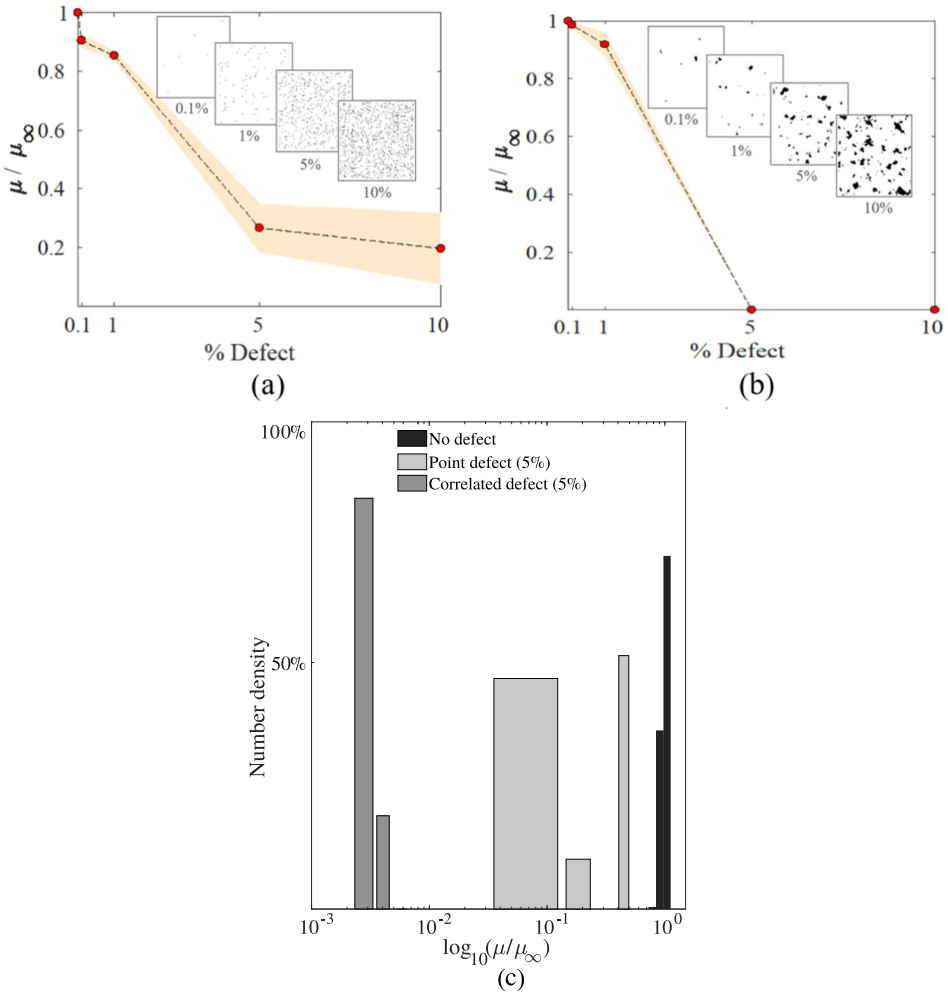

Fig. 4 Carrier mobility as a function of density of (a) **point defects and** (b) **structural defects in a model morphology.** The mobility was non-dimensionalized with respect to the mobility of perfect morphology with no defects. In (**b**), an average domain size of ~5% of total domain size was taken for 5% and 10% defect ratio. The inter/intra-chain hopping ratio is the same as in Fig. 3. The insets in show representative defect distribution for (**a**) uncorrelated and (**b**) correlated defects. Finally, we show a representative result that illustrates the relative impact of correlated versus uncorrelated defects. Up to a certain density of defects (around 5%), correlated and uncorrelated defects result in similar charge transport behavior. Beyond this point, correlated defects produce a larger degradation in mobility.

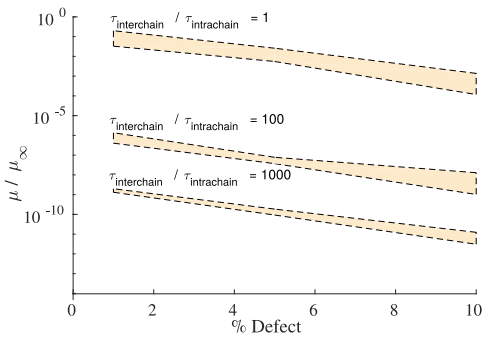

Fig. 5 A comprehensive view of the effect of defect density and inter/intra-chain hopping ratio on effective mobility. Each data point represents statistically averaged results across 500 model morphologies. The figure represents ~15,000 simulations.

DISCUSSION

In this work, we presented a computationally efficient route to model the charge mobilities in organic solids. We applied this model to semiconducting polymers by converting the spatial distribution of the polymer chains into a set of graph nodes and edges. Our model used physically meaningful weights for the graph edges in terms of the relative probability of charge hopping and the morphology of the system. Then, we utilized fast, well established algorithms to efficiently qualify the graph in terms of a representative mobility. The technique is simultaneously computationally efficient, both in terms of speed and memory, and extensible to incorporate other phenomena with minimal effort. The model shows that experimentally observed correlations between the charge carrier mobility and average morphologies can be reproduced with this relatively coarse grain model. The modularity of the approach provides a means to use alternative schemes to model the weights of the graph edges, i.e. electronic couplings. Furthermore, the model predicts the dependence of charge mobility on critical defects for model morphologies and variation in the inter and intra-chain transport. This approach provides a computationally efficient method to leverage structural analysis of semiconducting polymers by methods such as electron microscopy[5,7,10]. We expect that coupling nanoscale structural data with information about the distribution of size of polymer chains will provide important constraints for modeling charge transport.

METHODS

Constructing a graph-representation of morphology

Because charge transport is path dependant and directional, posing the problem as a graph enables fast and robust calculations. This method requires converting a microstructure image into a set of nodes and edges connecting the nodes. We consider the microstructure as composed of a distribution of semi-flexible polymer chains. Each semi-flexible polymer chain is represented as a chain of short connected rods, with each rod representing the local orientation of the backbone of the corresponding polymer chain. We convert this collection of rods into an equivalent graph representation[39,42]. Here, each rod is represented as a node (or a set of nodes arranged in order). Charge transport can then be framed as hopping over the nodes of the graph, with the frequency (or intensity) of hopping mediated by the strength (i.e. weight) of the edges between the vertices.

A graph $G(V, E)$ is defined by a set of nodes, V, and edges, E connecting the nodes. Two nodes are said to be connected if there exists an edge with non-zero weight between them. Thus, nodes roughly correspond to sites where the charge hopping can potentially change direction, and molecules. From a given site, the set of all directly accessible sites are connected with edges to that site. While the presence of an edge indicates just the accessibility, we weigh each edge that indicates the degree of accessibility. Hence, we construct a directed and weighted graph representation of the given morphology to explore transport characteristics. The details of the construction of this graph will follow next.

Assigning nodes. The first stage to converting into a graph is to define nodes, representative of sites of hopping. Depending on the type of polymer molecule, each polymer chain is divided into equally spaced nodes. In our work, the polymer chains we have are roughly of length 17 nm and we add a node every 1 nm apart. These parameters were chosen to represent the typical contour length of a semiconducting polymer, like poly(3-hexylthiophene), and the size of a typical monomer. The next stage is to find neighborhood (add edges) and assign relevant weights to these edges.

Finding neighborhood. From a given site, the charges can travel to, broadly speaking, two different kinds of sites—those within the same chain (intra-chain) and those in adjacent chains (inter-chain). Intra-chain neighbors can be easily determined by relative positions of the nodes on the given chain. In order to identify inter-chain neighbors, we use representative orbital overlaps. The electron cloud distribution around each molecular backbone is represented with a cylindrical/ellipsoidal annulus spanning the length of contour. If there is any intersection of these representative electron clouds between adjacent molecules, then all the sites belonging to these adjacent molecules are considered neighbors. It should be noted that while we represent all the nodes of adjacent molecules to be adjacent/neighbors, the transfer rates across these neighbors is not equal. This requires assigning weights to each of these graph edges, which will be discussed next.

Assigning weights to edges. Weights are assigned to the above identified edges (neighborhood) to distinguish different rates of transfer along different edges. Edges with higher weights have higher time for transfer across nodes, i.e., lower transfer rate. The base transfer rate is normalized to 1 (fastest), and this happens for an intra-chain hop within crystalline regions. The transfer rate in amorphous regions is several orders of magnitude lower than the transfer rate in crystalline regions. There are several other factors like orbital overlap between chains, relative orientation of monomers within a chain, relative orientation of chains, distances between hopping sites and direction of electric field. In other words, the qualitative and quantitative details of charge transfer rates is conveyed to the model through a careful choice of these weights. In this study, only the following factors are considered in calculation of weights to edges:

1. *Type of regions i.e. crystalline or amorphous*, w_r: The first classification of edges is done through classifying the chain to be belonging to amorphous or crystalline regions. Due to the alignment of the chains in crystalline regions, charge hops are considerably faster than over amorphous regions. Thus, edges belonging to crystalline region are given a weight of 1 and those in amorphous regions are given a large weight (1000 in our analysis). These edges are identified by tagging the nematic sticks during the morphology generation process. Please refer to the Supplementary information for more details.
2. *Type of edge—Intrachain vs. Interchain*, w_e: The ease of charge transfer within a chain is much higher than across different chains. Hence, inter-chain edges have a constant factor (≈100 in our work) edge weight multiplication compared to intra-chain edges.
3. *Effective orbital overlap between chains*, w_{ov}: The rate of charge transfer increases when the neighboring chains are perfectly aligned and there is greatest overlap of the molecular orbitals. Since we mathematically represent the orbitals as 'ellipsoidal' regions around the backbone, we quantify the effective overlap through intersection of these ellipsoids. Quantitatively, the edge weight between overlapping chains is considered to be inverse of the fraction of maximum overlap possible. Thus a fully overlapping set of chains have a weight of 1 (fastest hop rate) while chains with smallest overlap have a much larger weight, with zero overlapping chains with infinite weight.
4. *Relative orientation of chains*, w_{or}: Neighboring chains with different orientation of the backbone axis (for e.g. grain boundaries and amorphous regions) have significantly lower charge transfer rate compared to a pure crystal. We model this effect of orientation as $w_{or} = f(\cos(\theta))$, where θ shows the difference between orientation of adjacent chains. This formulation naturally models high charge transfer for parallel chains and no charge transfer across mutually perpendicular backbones.
5. *Distance between hopping sites*, w_d: When adjacency is calculated between chains, the representative nodes in the adjacent chains are not quantified in terms of the relative distance between the chains. This factor enables higher charge transfer rate for closer nodes in adjacent chains while simultaneously penalizes charge transfer between farther nodes. Several formulations can be considered to model this effect, like an exponential or linear decay with distance. In this work, we use a linear variation of the edge weight with distance between (adjacent) nodes.
6. *Direction of electric field*, w_f: The probability of charges flowing against the electric field is much lower compared to the probability of charges flowing along the external electric field. Hence edges which are aligned against the electric field have a constant, high factor (≈100 in our work). So, for two nodes connected by an edge, the weight against the electric field is 100 times the weight along the electric field.

The effect of all these factors on the overall charge transfer rate between nodes are considered multiplicative in this work. Hence, the effective edge weight between nodes i and j in the constructed graph is given by $w^{i,j} = w_r^{i,j} \times w_e^{i,j} \times w_{ov}^{i,j} \times w_{or}^{i,j} \times w_d^{i,j} \times w_f^{i,j}$.

Analytical determination of weights. The above method for assigning weights to the edges are useful to understand trends in mobility changes with several factors like electric field, orientation mismatch and grain boundaries. The weights could be assigned by other methods to capture differences in hopping events expected by different models, e.g. Miller–Abrahams or Marcus-type rate constants. Direct comparison of the graph-approach here to kinetic Monte Carlo simulations will require careful consideration of the behavior of the weights relative to expectations from the rate constants for hopping events. Because the calculations in the presented framework use normalized weights, the hopping rates from kMC need to be normalized such that the weight for the highest hopping rate is 1 and for every other edge is greater than 1. This will ensure longer duration of transport for edges related to lower hopping rate.

Calculating mobility

After constructing a graph from molecular information, as described above, we calculate a representative effective mobility of the system. We base our methodology on the observation that the most probable/preferred pathway for electronic transport is the shortest path from the origin to the destination electrode. So, given a graph representation of the morphology, we first assign electrodes and then calculate the shortest distances between each pair of electrode nodes. We use the well-known Dijkstra's algorithm[43] to find the shortest path. The weights of the edges as calculated above. As it can be understood, the weights are assigned such that edges with lower probability of charge transport are given higher weights. Once the shortest paths are calculated, the actual path distance is used to calculate the time of travel of a charge from one electrode to the other electrode. The mobility is then calculated as the inverse of the cumulative of the edge weights belonging to the shortest path. Paths with higher total cumulative edge weights pass through low charge hop probability sites. Consequently, these will have lower mobilities compared to paths that have lower cumulative edge weights. By

considering pairs of nodes across the morphology, a distribution of mobilities is constructed. This distribution is depicted in Figs. 1–5.

Assumption and extensions

In this section, we discuss assumptions made in the model and lay out approaches for relaxing these assumptions. We also identify natural extensions to the framework, which is easy to do due to the simplicity of the graph-based formulation.

Beyond single component system. While we focus on a single component material, the framework can be easily extended to consider multi-component organic blends. This change will require assigning different sets of edge weights (to reflect different hopping rates) across different materials. Additionally, one could go beyond pair-wise determination of the edge weights and assign edge weights based on the local neighborhood (coordination, local field, etc.).

Relaxation dynamics. The mechanism of charge motion at the molecular scale requires consideration of how the hopping rate depends on features such as relaxation (e.g. polaron formation) and the impact of neighbors. While we utilize averaged values based on typical behavior of polymers for the edge weights, it is relatively straightforward to incorporate more complex assignments of the edge weights from detailed electronic calculations.

Temperature dependence. The temperature dependence of transport in polymers at low carrier density generally follows activated transport when measured at macroscopic scales, i.e. large relative to the size of individual ordered regions. The addition of weights that depend on predictions for temperature activated jumps would provide a means to examine the overall behavior as a function of temperature.

Variations in site energy, and traps. It is conceptually straightforward to account for variations in site energy and distribution of traps via tailoring the edge weights across the graph. The addition of such effects would have comparable effects to the defects considered in Fig. 4 although the detailed impact would depend on the change in weights for hopping across such sites.

Exploring impact of tie chains and other morphological features. Transport along an extended tie chain in the background of amorphous chains would lead to comparable intrachain transport as we discuss in the "Introduction" section. One can use the graph model to examine specific cases, e.g. addition of different lengths of chains, for a given morphology. All one would need is a morphology generator (a non-trivial task) that can create appropriately features morphologies that can be input into the graph model discussed here.

DATA AVAILABILITY

The data used in the presented study are available upon request from the corresponding author.

CODE AVAILABILITY

The code used in the presented study are available upon request from the corresponding author.

Received: 28 June 2021; Accepted: 18 January 2022;
Published online: 11 March 2022

REFERENCES

1. Noriega, R. et al. A general relationship between disorder, aggregation and charge transport in conjugated polymers. *Nat. Mater.* **12**, 1038–1044 (2013).
2. Fratini, S., Nikolka, M., Salleo, A., Schweicher, G. & Sirringhaus, H. Charge transport in high-mobility conjugated polymers and molecular semiconductors. *Nat. Mater.* **19**, 491–502 (2020).
3. Coropceanu, V. et al. Charge transport in organic semiconductors. *Chem. Rev.* **107**, 926–952 (2007).
4. Baranovskii, S. D. Theoretical description of charge transport in disordered organic semiconductors: charge transport in disordered organic semiconductors. *Phys. Status Solidi (b)* **251**, 487–525 (2014).
5. O'Hara, K. et al. Effect of alkyl side chains on intercrystallite ordering in semiconducting polymers. *Macromolecules* **52**, 2853–2862 (2019).
6. Brinkmann, M. & Rannou, P. Molecular weight dependence of chain packing and semicrystalline structure in oriented films of regioregular poly(3-hexylthiophene) revealed by high-resolution transmission electron microscopy. *Macromolecules* **42**, 1125–1130 (2009).
7. Takacs, C. J., Brady, M. A., Treat, N. D., Kramer, E. J. & Chabinyc, M. L. Quadrites and crossed-chain crystal structures in polymer semiconductors. *Nano Lett.* **14**, 3096–3101 (2014).
8. Takacs, C. J. et al. Remarkable order of a high-performance polymer. *Nano Lett.* **13**, 2522–2527 (2013).
9. Fischer, F. S. U., Kayunkid, N., Trefz, D., Ludwigs, S. & Brinkmann, M. Structural models of poly (cyclopentadithiophene-*alt*-benzothiadiazole) with branched side chains: impact of a single fluorine atom on the crystal structure and polymorphism of a conjugated polymer. *Macromolecules* **48**, 3974–3982 (2015).
10. Panova, O. et al. Diffraction imaging of nanocrystalline structures in organic semiconductor molecular thin films. *Nat. Mater.* **18**, 860–865 (2019).
11. Wirix, M. J., Bomans, P. H., Friedrich, H., Sommerdijk, N. A. & de With, G. Three-dimensional structure of p3ht assemblies in organic solvents revealed by cryo-tem. *Nano Lett.* **14**, 2033–2038 (2014).
12. Collins, B. et al. Polarized x-ray scattering reveals non-crystalline orientational ordering in organic films. *Nat. Mater.* **11**, 536 (2012).
13. Carpenter, J. H. et al. Competition between exceptionally long-range alkyl sidechain ordering and backbone ordering in semiconducting polymers and its impact on electronic and optoelectronic properties. *Adv. Funct. Mater.* **29**, 1806977 (2019).
14. Vakhshouri, K. et al. Signatures of intracrystallite and intercrystallite limitations of charge transport in polythiophenes. *Macromolecules* **49**, 7359–7369 (2016).
15. Hsu, B. B.-Y. et al. The density of states and the transport effective mass in a highly oriented semiconducting polymer: electronic delocalization in 1d. *Adv. Mater.* **27**, 7759–7765 (2015).
16. Kilina, S. et al. Electronic structure of self-assembled amorphous polyfluorenes. *ACS Nano* **2**, 1381–1388 (2008).
17. Vukmirović, N. & Wang, L.-W. Density of states and wave function localization in disordered conjugated polymers: a Large Scale Computational Study. *J. Phys. Chem. B* **115**, 1792–1797 (2011).
18. McMahon, D. P. et al. Relation between microstructure and charge transport in polymers of different regioregularity. *J. Phys. Chem. C* **115**, 19386–19393 (2011).
19. Gemünden, P., Poelking, C., Kremer, K., Daoulas, K. & Andrienko, D. Effect of mesoscale ordering on the density of states of polymeric semiconductors. *Macromol. Rapid Commun.* **36**, 1047–1053 (2015).
20. van der Kaap, N. & Koster, L. Massively parallel kinetic Monte Carlo simulations of charge carrier transport in organic semiconductors. *J. Comput. Phys.* **307**, 321–332 (2016).
21. Upreti, T. et al. Experimentally validated hopping-transport model for energetically disordered organic semiconductors. *Phys. Rev. Appl.* **12**, 064039 (2019).
22. Li, H., Li, Y., Li, H. & Brédas, J.-L. Organic field-effect transistors: a 3d kinetic monte carlo simulation of the current characteristics in micrometer-sized devices. *Adv. Funct. Mater.* **27**, 1605715 (2017).
23. Fornari, R. P., Blom, P. W. & Troisi, A. How many parameters actually affect the mobility of conjugated polymers? *Phys. Rev. Lett.* **118**, 086601 (2017).
24. Jackson, N. E. Coarse-graining organic semiconductors: the path to multiscale design. *J. Phys. Chem. B* **125**, 485–496 (2021).
25. Pearson, D. S., Pincus, P. A., Heffner, G. W. & Dahman, S. J. Effect of molecular weight and orientation on the conductivity of conjugated polymers. *Macromolecules* **26**, 1570–1575 (1993).
26. Rudnicki, P. E. et al. Impact of liquid-crystalline chain alignment on charge transport in conducting polymers. *Macromolecules* **52**, 8932–8939 (2019).
27. Segatta, F., Lattanzi, G. & Faccioli, P. Predicting charge mobility of organic semiconductors with complex morphology. *Macromolecules* **51**, 9060–9068 (2018).
28. O'Connor, B. T. et al. Morphological origin of charge transport anisotropy in aligned polythiophene thin films. *Adv. Funct. Mater.* **24**, 3422–3431 (2014).
29. Gu, K. & Loo, Y.-L. The polymer physics of multiscale charge transport in conjugated systems. *J. Polym. Sci. Part B* **57**, 1559–1571 (2019).
30. Mollinger, S. A., Krajina, B. A., Noriega, R., Salleo, A. & Spakowitz, A. J. Percolation, tie-molecules, and the microstructural determinants of charge transport in semicrystalline conjugated polymers. *ACS Macro Lett.* **4**, 708–712 (2015).
31. Gu, K. et al. Assessing the Huang–Brown description of tie chains for charge transport in conjugated polymers. *ACS Macro Lett.* **7**, 1333–1338 (2018).
32. Greco, C., Melnyk, A., Kremer, K., Andrienko, D. & Daoulas, K. C. Generic model for lamellar self-assembly in conjugated polymers: linking mesoscopic morphology and charge transport in p3ht. *Macromolecules* **52**, 968–981 (2019).
33. Li, H., Sini, G., Sit, J., Moulé, A. J. & Bredas, J.-L. Understanding charge transport in donor/acceptor blends from large-scale device simulations based on experimental film morphologies. *Energy Environ. Sci.* **13**, 601–615 (2020).

34. Liu, F., van Eersel, H., Bobbert, P. A. & Coehoorn, R. Three-dimensional modeling of bipolar charge-carrier transport and recombination in disordered organic semiconductor devices at low voltages. *Phys. Rev. Appl.* **10**, 054007 (2018).
35. Vehoff, T., Baumeier, B., Troisi, A. & Andrienko, D. Charge transport in organic crystals: role of disorder and topological connectivity. *J. Am. Chem. Soc.* **132**, 11702–11708 (2010).
36. Savoie, B. M. et al. Mesoscale molecular network formation in amorphous organic materials. *Proc. Natl Acad. Sci. USA* **111**, 10055–10060 (2014).
37. Jackson, N. E., Savoie, B. M., Chen, L. X. & Ratner, M. A. A simple index for characterizing charge transport in molecular materials. *J. Phys. Chem. Lett.* **6**, 1018–1021 (2015).
38. Baumeier, B., Stenzel, O., Poelking, C., Andrienko, D. & Schmidt, V. Stochastic modeling of molecular charge transport networks. *Phys. Rev. B* **86**, 184202 (2012).
39. West, D. B. et al. *Introduction to Graph Theory*, Vol. 2 (Prentice-Hall, 1996).
40. Wodo, O., Tirthapura, S., Chaudhary, S. & Ganapathysubramanian, B. A graph-based formulation for computational characterization of bulk heterojunction morphology. *Org. Electron.* **13**, 1105–1113 (2012).
41. Van, E., Jones, M., Jankowski, E. & Wodo, O. Using graphs to quantify energetic and structural order in semicrystalline oligothiophene thin films. *Mol. Syst. Design Eng.* **3**, 853–867 (2018).
42. Balaban, A. T., Brocas, J. & Dubois, J. -E. *Chemical Applications of Graph Theory*, Vol. 185 (Academic Press, 1976).
43. Dijkstra, E. W. A note on two problems in connexion with graphs. *Numer. Math.* **1**, 269–271 (1959).
44. Dantzig, G. & Fulkerson, D. R. On the max flow min cut theorem of networks. *Linear Inequal. Relat. Syst.* **38**, 225–231 (2003).
45. Carbone, P. & Troisi, A. Charge diffusion in semiconducting polymers: analytical relation between polymer rigidity and time scales for intrachain and interchain hopping. *J. Phys. Chem. Lett.* **5**, 2637–2641 (2014).
46. Nahid, M. M. et al. Unconventional molecular weight dependence of charge transport in the high mobility n-type semiconducting polymer p (ndi2od-t2). *Adv. Funct. Mater.* **27**, 1604744 (2017).
47. Patel, S. N. et al. Morphology controls the thermoelectric power factor of a doped semiconducting polymer. *Sci. Adv.* **3**, e1700434:1–13 (2017).
48. Roberts, A. P. Statistical reconstruction of three-dimensional porous media from two-dimensional images. *Phys. Rev. E* **56**, 3203 (1997).

ACKNOWLEDGEMENTS

This work was supported in part through NSF 1906194, and the ONR MURI. E.L. received support from a National Science Foundation Graduate Research Fellowships (DGE-1144085).

AUTHOR CONTRIBUTIONS

E.L. contributed to data generation and comparison with existing literature. R.N. contributed to model development, implementation and analysis. B.S.S.P. contributed to problem formulation, model development, analysis and comparison. M.L.C. and B.G. contributed to problem formulations and project oversight. R.N., E.L., B.S.S.P., M.L.C. and B.G. contributed to manuscript preparation.

COMPETING INTERESTS

The authors declare no competing interests.

ADDITIONAL INFORMATION

Supplementary information The online version contains supplementary material available at https://doi.org/10.1038/s41524-022-00714-w.

Correspondence and requests for materials should be addressed to Michael L. Chabinyc or Baskar Ganapathysubramanian.

Reprints and permission information is available at http://www.nature.com/reprints

Publisher's note Springer Nature remains neutral with regard to jurisdictional claims in published maps and institutional affiliations.